Picozzi, M., Bindi, D., Brondi, P., DiGiacomo, D., Parolai, S., Zollo, A. (2017): Rapid determination of P wave-based energy magnitude: Insights on source parameter scaling of the 2016 Central Italy earthquake sequence. - *Geophysical Research Letters*, *44*, 9, pp. 4036—4045.

DOI: http://doi.org/10.1002/2017GL073228

AGU PUBLICATIONS

Geophysical Research Letters

RESEARCH LETTER
10.1002/2017GL073228

Key Points:
- An energy-based local magnitude scale (M_{Le}) for measuring the earthquake size during real-time operations is proposed
- In the analysis of the 2016 Central Italy sequence, large values for the apparent stress are observed, extending from about 0.5 to 25 MPa
- M_w and M_{Le} can be used together for better capturing the shaking potential of earthquakes in real-time applications

Supporting Information:
- Supporting Information S1

Correspondence to:
M. Picozzi,
matteo.picozzi@unina.it

Citation:
Picozzi, M., D. Bindi, P. Brondi, D. Di Giacomo, S. Parolai, and A. Zollo (2017), Rapid determination of *P* wave-based energy magnitude: Insights on source parameter scaling of the 2016 Central Italy earthquake sequence, *Geophys. Res. Lett.*, *44*, 4036–4045, doi:10.1002/2017GL073228.

Received 23 FEB 2017
Accepted 26 MAR 2017
Accepted article online 29 MAR 2017
Published online 6 MAY 2017

Rapid determination of *P* wave-based energy magnitude: Insights on source parameter scaling of the 2016 Central Italy earthquake sequence

Matteo Picozzi[1], Dino Bindi[2], Piero Brondi[1], Domenico Di Giacomo[3], Stefano Parolai[2], and Aldo Zollo[1]

[1]Department of Physics, Università di Napoli Federico II, Naples, Italy, [2]GFZ German Research Centre for Geosciences, Helmholtz Centre Potsdam, Potsdam, Germany, [3]International Seismological Centre, Thatcham, UK

Abstract We propose a *P* wave based procedure for the rapid estimation of the radiated seismic energy, and a novel relationship for obtaining an energy-based local magnitude (M_{Le}) measure of the earthquake size. We apply the new procedure to the seismic sequence that struck Central Italy in 2016. Scaling relationships involving seismic moment and radiated energy are discussed for the M_w 6.0 Amatrice, M_w 5.9 Ussita, and M_w 6.5 Norcia earthquakes, including 35 $M_L > 4$ aftershocks. The M_w 6.0 Amatrice earthquake shows the highest apparent stress, and the observed differences among the three main events highlight the dynamic heterogeneity with which large earthquakes can occur in Central Italy. Differences between estimates of M_{Le} and M_w allows identification of events which are characterized by a higher proportion of energy being transferred to seismic waves, providing important real-time indications of earthquakes shaking potential.

1. Introduction

In the framework of real-time seismology [*Kanamori*, 2005], the rapid determination of earthquake location and size can allow for the timely implementation of emergency plans and, under favorable conditions, early warnings may be issued. The earthquake size can be measured according to different magnitude scales which provide complementary information about the static and dynamic features of earthquake rupture [*Kanamori*, 1983; *Atkinson*, 1995; *Bormann et al.*, 2013]. For example, the moment magnitude M_w [*Kanamori*, 1977; *Hanks and Kanamori,* 1979], based on an estimate of the seismic moment [*Aki*, 1968; *Kanamori and Anderson*, 1975], provides fault-averaged, low-frequency information about the source processes, but relatively less information about the small-wavelength high-frequency rupture details [e.g., *Beresnev*, 2009]. For instance, *Baltay et al.* [2013] observed that for the same M_w, earthquakes with larger stress drop can give rise to larger ground motion, and therefore, they suggested that rapid estimates of the stress drop can allow more reliable predictions of the earthquake shaking.

Here we follow the approach of *Atkinson and Hanks* [1995], which complemented M_w with a new magnitude scale, based on the high-frequency level of the Fourier spectrum, to provide a complete description of the ground motion over the entire frequency range of engineering interest. Following their suggestion, another possibility is to consider the energy magnitude M_e [*Choy and Boatwright,* 1995; *Choy and Kirby*, 2004]. Since M_e is based on an estimate of the radiated energy E_R, it is linked to the source dynamics and is more sensitive to high-frequency source details (e.g., variations of the slip and/or stress conditions, and the dynamic friction at the fault surface during the rupture process). M_e was introduced by *Choy and Boatwright* [1995] using teleseismic broadband *P* wave recordings and an automatic procedure for its estimation is available [*Di Giacomo et al.*, 2010]. At local distances, several approaches for computing E_R have been proposed [e.g., *Thatcher and Hanks*, 1973; *Cocco and Rovelli*, 1989; *Kanamori et al.*, 1993; *Singh and Ordaz*, 1994]. In these studies, E_R was computed from *S* wave signals corrected for a suitable parametric attenuation model [e.g., *Kanamori et al.*, 1993], or from a source spectrum that was obtained by jointly inverting a set of local recordings for the source, attenuation, and site contributions [e.g., *Zollo et al.*, 2014].

Our aim is to present a new procedure for estimating the earthquake size within the framework of real-time seismology. For this reason, the procedure relies only on the analysis of early-recorded *P* wave signals. We consider M_e rather than M_w because it more accurately represents the shaking potential of an earthquake

[*Choy and Boatwright*, 1995]. We estimate E_R from the IV2 parameter [*Festa et al.*, 2008; *Brondi et al.*, 2015] computed for *P* waves. The energy values are then used to define a new magnitude scale. At teleseismic distances, *Choy and Boatwright* [1995] defined M_e to be compatible with the surface wave magnitude, while at local distances we opt for the local magnitude M_L. The rationale behind this choice is based on four arguments: (a) M_L is routinely computed by local networks, often based on local attenuation models; (b) for $M_L \leq 6$, it is expected to scale with the logarithm of E_R [e.g., *Kanamori et al.*, 1993; *Mereu*, 2017]; (c) M_L depends on stress drop and average rupture velocity [*Deichmann*, 2017]; and (d) previous studies found that M_L allows for reduction of the between-event variability for frequencies above 1 Hz when calibrating ground motion prediction equations for moderate size earthquakes [e.g., *Bindi et al.*, 2007].

The proposed new methodology is discussed, taking Central Italy as a region representative of areas where the influence of seismic hazard on the residential building codes is dominated by close-distance earthquakes of low-to-moderate magnitude (i.e., from 4.5 to 6.5) [*Barani et al.*, 2009]. We first calibrate the attenuation of E_R with distance and derive an empirical relationship between M_L and E_R, considering 29 earthquakes with $M_w > 4$ belonging to the L'Aquila (2009) seismic sequences in Central Italy, and to the Emilia (2012) sequence in Northern Italy. Then, the procedure is applied to 38 earthquakes of the 2016, Central Italy, seismic sequence. Finally, the estimates of E_R are used to discuss dynamic characteristics of the rupture process which are relevant to the 2016 sequence.

2. Data Set

We use data recorded by the Italian strong motion network (RAN) managed by the Department of Civil Protection (DPC), as well as data recorded by permanent and temporary stations of the Italian National Seismic Network operated by the National Institute for Geophysics and Volcanology (INGV). Lastly, we include data available from the Enea Network (i.e., Agenzia Nazionale per le Nuove Technolgie). The manually revised strong motion data are distributed through the ITACA 2.0 portal [*Luzi et al.*, 2008; *Pacor et al.*, 2011]. The data set used to calibrate the attenuation model between the squared-velocity parameter IV2 and E_R, as well as the scaling between E_R and M_L, are composed of 29 events (Figure 1a and Table S1 in the supporting information) belonging to two main seismic sequences which occurred recently in Italy: the 2009 L'Aquila sequence [*Ameri et al.*, 2009] and the 2012 Emilia sequence [*Luzi et al.*, 2013]. The calibration data set includes 888 recordings with M_L between 4 and 6.1, obtained from 221 stations located at hypocentral distances smaller than 100 km (Figure 1b). To reproduce a rapid procedure, the recordings are preprocessed following the steps proposed by *Zollo et al.* [2006] which are appropriate for simulating the performance of rapid earthquake analyses (see Text S1 for details).

The empirical relationships obtained in this study are applied to the 2016 August–October, Central Italy, earthquake sequence which includes clusters of moderate to strong earthquakes. We consider 1840 recordings from 38 earthquakes (Table S2) that occurred between 24 August and 11 November 2016. The data set includes the M_w 6.0 Amatrice, the M_w 5.9 Ussita, and the M_w 6.5 Norcia main shocks that occurred on 24 August, 26 October, and 30 October, respectively [*Gruppo di lavoro INGV*, 2016]. On average, the 2016 sequences have been recorded by 40 RAN stations within 100 km from the epicenter (Figures 1a and 1c).

3. IV2 Versus Radiated Energy

In this study, we develop an empirical relationship between IV2 and E_R. Following *Izutani and Kanamori* [2001], we estimate E_R for the 29 earthquakes in the calibration data set by computing the theoretical *Brune's* [1970] spectrum for *P* and *S* waves. We use the source parameters of the calibration earthquakes (i.e., corner frequency f_c, seismic moment M_0, and stress drop $\Delta\tau_s$) as estimated by *Bindi et al.* [2004, 2009] and *Castro et al.* [2013]. We relate IV2 estimated for each recording to the source size expressed in terms of E_R, computed from the theoretical Brune's spectrum assuming a linear model where the attenuation with distance is expressed in a nonparametric form; that is,

$$\log_{10}[\mathrm{IV2}(R_H)] = A + B\log_{10}(E_R) + w_j C_j + \left(1 - w_j\right) C_{j+1} \tag{1}$$

where the hypocentral distance range is discretized into N_{bin}; the index $j = 1, \ldots, N_{\mathrm{bin}} + 1$ indicates the jth node selected such that the hypocentral distance R_H is between the distances $r_j \leq R_H < r_{j+1}$; the attenuation

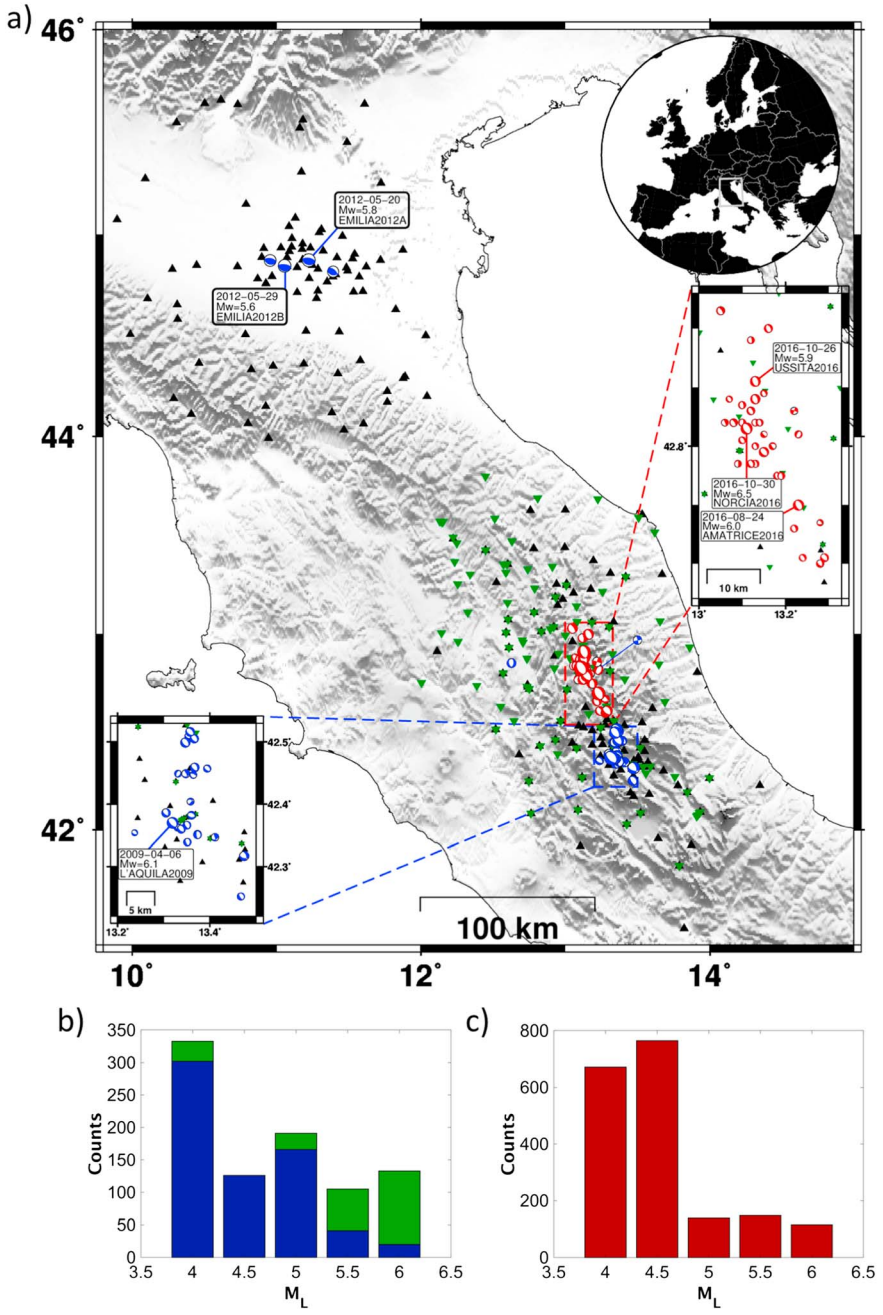

Figure 1. (a) Map of the calibration data set for the 2009 L'Aquila (blue) and 2012 Emilia (green) sequences and test data set of the 2016 Central Apennines sequence (red). Calibration data set stations (black triangles) and test data set ones (green inverted triangles) are shown. (b) Number of recordings for magnitude class for the calibration data set (blue and green for the 2009 L'Aquila and 2012 Emilia sequences, respectively). (c) The same as Figure 1b but for the testing data set.

function is linearized between nodes r_j and r_{j+1} using the weights w, computed as $w_j = (r_{j+1} - R_H)/(r_{j+1} - r_j)$. In this study, the hypocentral distance range 0–100 km is discretized into 20 bins with equal width (i.e., 5 km). The coefficients A, B, C_j of the model are determined by solving equation (1) in a least squares sense and, to remove the trade-off between source and attenuation terms, the coefficient C_2 (i.e., the attenuation at 10 km) is constrained to zero.

To increase the number of recordings for magnitude between 5 and 6, the calibration data set includes 655 recordings relevant to the 2009 L'Aquila sequence and 233 recordings for the 2012 Emilia sequence (Figures 1b and 1c). While we assume that the source scaling in equation (1) is the same for the two sequences (i.e., parameters A and B), previous studies highlighted peculiarities in the attenuation with distance for the recordings of the Emilia sequence [*Lanzano et al.*, 2016]. Therefore, equation (1) is modified by introducing two different sets of attenuation coefficients: C_j^{NI}(where NI stands for Northern Italy) and C_j^{CI} (where CI stands for Central Italy) for Emilia and L'Aquila recordings, respectively. The obtained coefficients A, B, C_j^{NI}, and C_j^{CI} of equation (1) are reported in Table S3. The calculated regression has a R^2 correlation coefficient equal to 0.82 and standard deviation of 0.51 which is consistent with the uncertainty on regression coefficients from the M_w versus IV2 empirical laws derived by *Festa et al.* [2008] and *Lancieri et al.* [2011].

Figure S1a compares the observed IV2 values, corrected for attenuation effects as modeled through the C_j^{NI} and C_j^{CI} coefficients, with E_R. The source scaling (black line) defined by the A and B coefficients in equation (1) capture well the trend in the data over the entire energy range for both the Emilia and Central Italy regions. The distance scaling of model (1) is shown in Figure S1b where the distance distribution of the observed IV2 values, corrected for the source scaling $A + B\log_{10}(E_R)$, are compared with the attenuation models C_j^{NI} (green curve) and C_j^{CI} (blue curve). The good agreement with the corrected data confirms the suitability of the obtained attenuation models and highlights the importance of considering different regions within the model.

4. ML Versus E_R: An Energy-Based Local Magnitude

ML values for the 29 calibration earthquakes selected have been retrieved by the INGV and ITACA 2.0 databases (Table S1). We consider a linear model between ML and $\log_{10}(E_R)$, including an adjustment factor δ, over the offset α, to account for possible regional differences between the scaling in Northern and Central Italy:

$$\mathrm{ML} = \alpha + \beta\log_{10}(E_R) + \delta \tag{2}$$

δ is determined as random effect [*Bates et al.*, 2015]. The maximum likelihood solution is defined by $\alpha = (-1.817 \pm 0.360)$ and $\beta = (0.546 \pm 0.028)$, while the two δ are estimated to be -0.1182 and 0.1182 for Central and Northern Italy, respectively. The standard deviation of the residuals is 0.45. The obtained relationship is shown in Figure S1c, where the median models for the two regions are compared to the data, while Figure S1d shows that the overall residual distribution is unbiased. When applied to new E_R estimates, equation (2) provides a mean for obtaining an energy-based local magnitude (hereinafter referred to as M_{Le}) that, as discussed by *Kanamori et al.* [1993], agrees with ML for small earthquakes, but being based on a measure of the radiated energy can be extended toward larger magnitude while avoiding saturation.

5. Application to the 2016 Central Italy Sequences

The methodology proposed to compute M_{Le} is applied to 38 earthquakes occurred in Central Italy in 2016 (Table S2). To simulate real-time analysis and verify the time frame within which stable M_{Le} estimates can be obtained for the three larger earthquakes, the M_{Le} estimates are obtained by increasing progressively the numbers of stations in the E_R assessment according to their hypocentral distance (Figure 2a). In the application of the procedure, we assume that a location estimate is available from a separate algorithm (e.g., PRESTo [*Satriano et al.*, 2011; *Picozzi et al.*, 2015]), which allows for the automatic selection in real time of the P wave window and the coefficients for the correction of attenuation effects. The P wave windows are thus progressively increasing with epicenter distance to capture the whole source time duration and avoid magnitude saturation effects in case of large events [*Colombelli et al.*, 2012].

Since the uncertainty on E_R is used to compute the 95% confidence limits on M_{Le}, the uncertainty on MLe decreases with hypocentral distance (Figure 2a). The evolutionary M_{Le} estimates stabilize between about 45 km and about 60 km (i.e., between 8 and 10 s from the origin time), corresponding to about 15 and 20 stations and to a maximum P wave window of about 5.6 and 7.5 s, respectively. These results suggest that the procedure for estimating MLe may be useful for rapid earthquake analysis. It is worth noting that beyond the indicated distances, M_{Le} converges toward values close to the M_w provided by the INGV for Ussita (M_w 5.9)

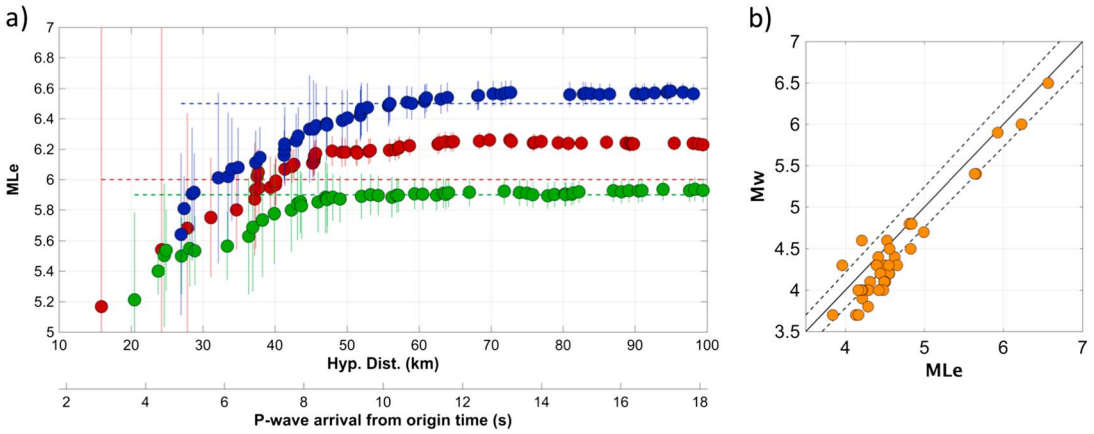

Figure 2. (a) Evolutionary estimation of M_{Le} with hypocentral distance for the Amatrice M_w 6.0 (red dots), the Ussita M_w 5.9 (green dots), and the Norcia M_w 6.5 earthquake (blue dots). Vertical bars indicate the range of uncertainty on M_{Le}. Includes M_w estimates colored horizontal dashed lines. (b) M_w versus M_{Le} (orange dots), the 1:1 line (black), and ±0.3 magnitude units (black dashed lines) are also plotted.

and Norcia (M_w 6.5) earthquakes (i.e., M_{Le} = 5.9 ± 0.08 and 6.6 ± 0.06, respectively), while in the case of the Amatrice (M_w 6.0) earthquake, M_{Le} is larger than M_w (i.e., M_{Le} = 6.2 ± 0.05). Regarding the Norcia (M_w 6.5) earthquake, M_{Le} converges to M_w, overcoming the saturation limit of M_L (i.e., M_L = 6.1). Teleseismic M_e estimates derived from the procedure proposed by *Di Giacomo et al.* [2010] agree with M_{Le} estimates in the case of Amatrice (M_e 6.16) and Norcia (M_e 6.5) earthquakes, while they are slightly higher in the case of the Ussita (M_e 6.2) event. Figure 2b shows the comparison between M_{Le} and M_w for the analyzed 38 events. For $M_w \leq 5$, most of the MLe overestimates M_w; for larger events, MLe tends to be on average slightly larger than M_w.

Figure 3a shows that E_R scales linearly with M_0. The best fit line obtained considering the entire seismic moment range is $\log_{10}(E_R) = 1.15 \log_{10}(M_0) - 5.99$, with a standard deviation equal to 0.35. A slope larger than 1 indicates that the ratio between E_R and M_0 increase with increasing M_0, suggesting a possible breakdown of the source scaling self-similarity. Indeed, when the fit is performed considering the earthquakes above and below M_w = 5 separately, a slope close to 1 is obtained for both ranges (i.e., $\log_{10}(E_R) = 1.03 \log_{10}(M_0) - 4.24$, with a standard deviation equal to 0.35, and, $\log_{10}(E_R) = 1.04 \log_{10}(M_0) - 4.15$, with a standard deviation equal to 0.16 below and above M_w = 5, respectively), but with different intercepts. As indicated by the isolines of apparent stress $\tau_a = \mu E_R/M_0$ (computed assuming a crustal shear modulus μ equal to $3.3 \cdot 10^4$ MPa), the average τ_a values for the small and large earthquakes are 5 and 10 MPa, respectively, although we observe that a subset of aftershocks are aligned on the same average value of the larger events. To get more insight into the source scaling properties, Figure 3b shows how the ratio between radiated seismic energy and seismic moment (i.e., E_R/M_0, also termed "scaled energy" [*Kanamori and Brodsky*, 2004]) varies with seismic moment. The scaled energy values found in this study are compared with those of *Kanamori et al.* [1993] and *Mayeda and Walter* [1996], both related to United States earthquakes, as well as with those of *Oth et al.* [2010] and *Oth* [2013] for crustal Japanese earthquakes with depths within 30 km. We observe that $M_w < 5$ earthquakes have scaled energy values in agreement with those of the Japanese earthquakes with higher stress drop.

It is noteworthy that a consistent number of $M_w < 5$ earthquakes show a scaled energy of the same order of magnitude as the three largest events (Figures 3a and 3b). This result suggests that the dynamics of faulting between the groups of small and large earthquakes in the Apennines sector has been, at first approximation, similar. On the other hand, when we consider the three larger magnitude events of the sequence (Figure 3b), we observe that for a similar M_0 the Amatrice M_w 6.0 event has a scaled energy significantly higher than the Ussita 5.9 M_w one (i.e., ~25 MPa and ~10 MPa, respectively). Moreover, the M_w 6.5 Norcia earthquake presents an intermediate scaled energy between the other two main shocks (i.e., ~ 20 MPa), but of the same order of the two M_w 5.4 aftershocks. The observed differences in terms of scaled energy between the larger earthquakes of the sequence highlight the heterogeneity of the dynamic mechanisms with which large magnitude earthquakes can occur in the Apennines, with implications for possible significant ground motion

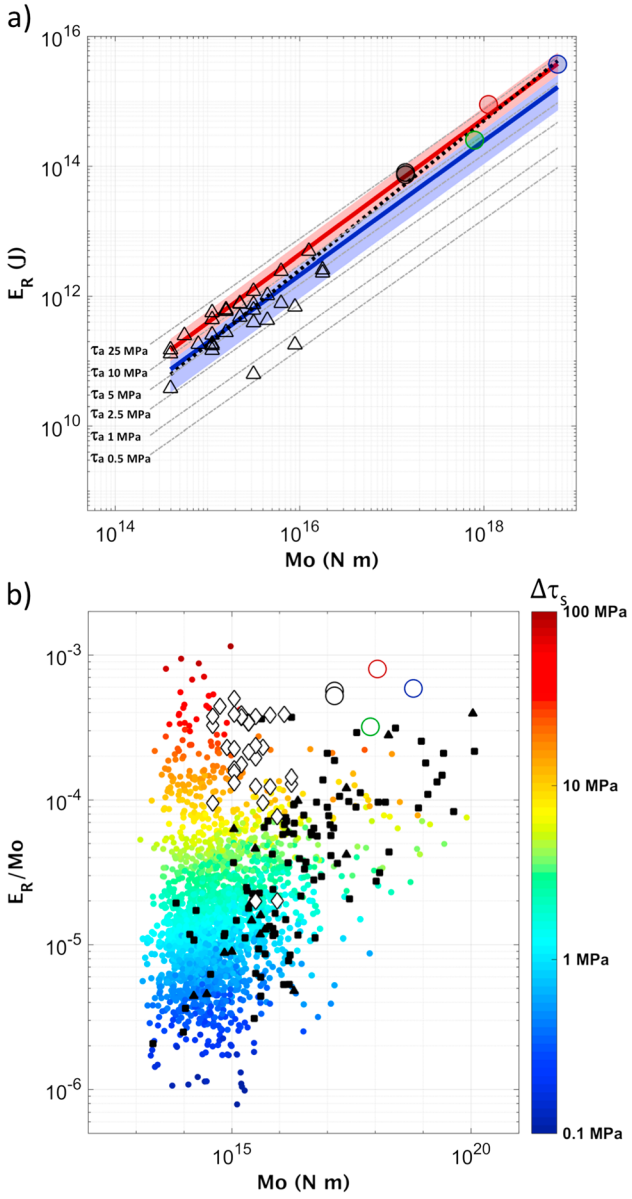

Figure 3. (a) M_0 versus E_R for events with $M_w < 5$ (triangles); two M_w 5.4 aftershocks (light black dot); Ussita M_w 5.9 (green dot), Amatrice M_w 6.0 (red dot), and Norcia M_w 6.5 (blue dot) main shocks. The best fit line for $M_w < 5$ events (blue) ± 1 standard deviation (light blue area), for $M_w > 5$ (red) ± 1 standard deviation (light red area), and for the whole data set (black dotted line) are shown as well. Lines of equal apparent stress are shown as gray dashed lines. (b) M_0 versus scaled energy for events of the 2016 Central Italy sequence with $M_w < 5$ (white diamonds) and with $M_w > 5$ (white circles). Results from *Kanamori et al.* [1993] (black triangles), *Mayeda and Walter* [1996] (black squares), and from *Oth et al.* [2010] and *Oth* [2013] (dots colored per static stress drop values) are also shown.

differences between events with similar M_w. Figure 4a shows that the between-event residuals δBe [*Al Atik et al.*, 2010] between observed PGA values and values predicted by the M_w-based attenuation model proposed for Italy by *Bindi et al.* [2011] linearly scale with the scaled energy (i.e., δBe = 0.48 E_R/M_0 ± 0.12). Interestingly, Figure 4b shows that when M_{Le} is used instead of M_w for the predictions, the between-event variability is reduced (i.e., δBe = 0.14 E_R/M_0 ± 0.13).

Figure 4c shows the differences between M_{Le} and M_w (i.e., $M_{Le} - M_w$) with respect to the apparent stress, τ_a (i.e., derived by the scaled energy assuming a constant μ equal to $3.3 \cdot 10^4$ MPa). Besides the 2016 Central Italy sequence, Figure 4c also includes the M_w 6.1, 2009, L'Aquila, and the M_w 5.0, 2013, Matese, earthquakes, which occurred in nearby areas within the Central Apennines. $M_{Le} - M_w$ linearly scales with τ_a as expected (i.e., all the involved measures are related to log (E_R) and log(M_0)), and events with different magnitude are aligned along parallel lines (i.e., for a fixed value of $M_{Le} - M_w$, τ_a increases with magnitude). The values of static stress drop shown as reference in Figure 4c are derived from τ_a, assuming the simplest idealized case of rupture, where the final average stress and the average stress during faulting are equal (i.e., Orowan's model) [*Orowan,* 1960]; that is, $\Delta\tau_s = 2\tau_a$.

6. Discussion and Conclusion

We envisage that similarly to the idea from *Di Giacomo et al.* [2008, 2010], at the global scale, our approach for estimating M_{Le} can be used for complementing M_w in real-time operations at the local scale. The difference between M_{Le} and M_w used for a rapid identification of events characterized by a higher amount of energy transferred to seismic waves (as shown in Figure 4c, where $M_{Le} - M_w > 0$) corresponds to events sharing the same M_w but having higher E_R. A similar strategy was proposed by *Atkinson and Hanks* [1995] considering a high-frequency magnitude and M_w, whose differences were found informative of the $\Delta\tau_s$ variability in the study areas.

The static stress drop for the three largest shocks obtained assuming the Orowan model vary from 20 MPa for the M_w 5.9, Ussita event to about 30 and 50 MPa for the Norcia (M_w 6.5) and Amatrice (M_w 6.0) earthquakes,

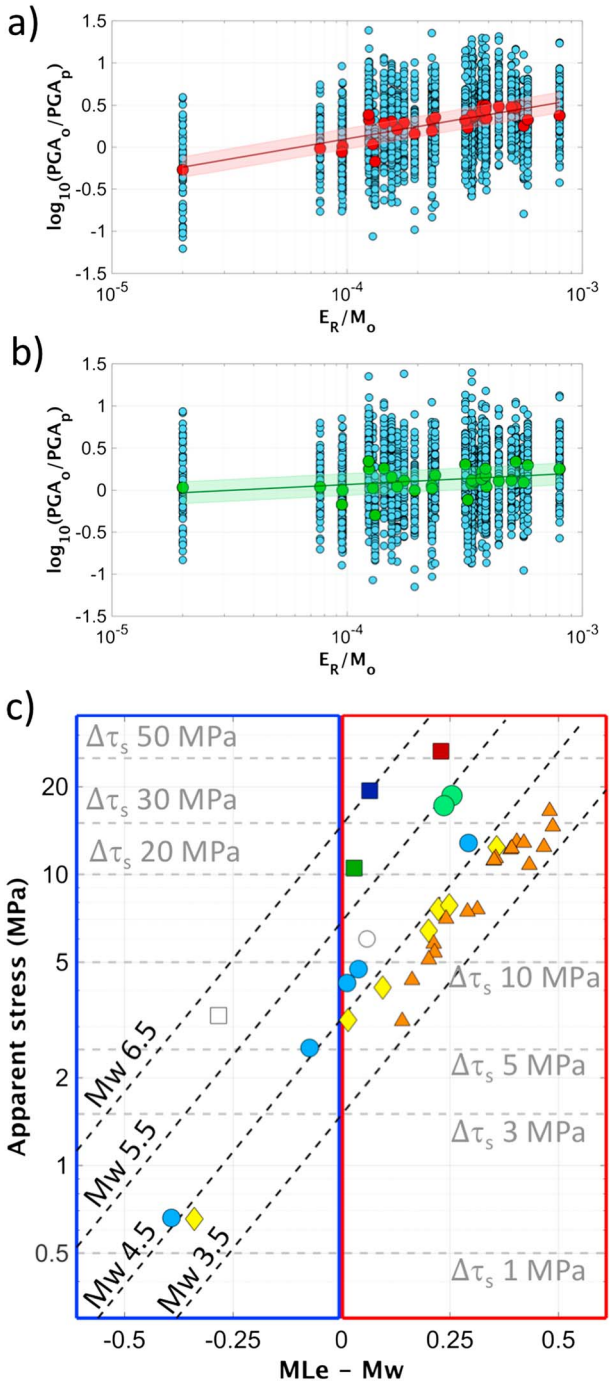

Figure 4. (a) Residuals between observed and predicted PGA using M_w (light blue circles) and between-event residuals (red circles) versus scaled energy, best fit line (red line), and ±1 standard deviation (light red area). (b) Same as Figure 4a but using M_{Le}, with between-event residuals and best fit line ±1 standard deviation (green circles and lines, respectively). (c) $M_{Le} - M_w$ versus apparent stress: 2016, M_w 6.0 Amatrice (red square); 2016, M_w 5.9 Ussita (green square); 2016 M_w 6.5 Norcia (blue square); 2009, M_w 6.3 L'Aquila 2009 (white square); 2013. M_w 5.0 Matese (white dot). Aftershocks of the 2016 Central Italy sequence: $M_w < 4.2$ (orange triangles); $4.2 <= M_w < 4.5$ (yellow diamonds); $4.5 <= M_w < 5$ (light blue dots); $5 <= M_w < 5.9$ (light green dots). Lines of equal M_w (dashed black) and equal static stress drop for the Orowan's model (dashed gray) are shown for the sake of comparison.

respectively (Figure 4c). However, if instead of the Orowan model we hypothesize that dynamic weakening occurred during the 2016 earthquakes the consequent negative overshoot (undershoot) would lead the $\tau_a/\Delta\tau_s$ ratio toward 1 [*Beeler et al.*, 2003], with static stress drop values smaller than those obtained by from Orowan's model. *Malagnini et al.* [2008, 2010] showed evidence of dynamic weakening in the case of the 1997–1998 Colfiorito earthquake sequence (Apennines, Central Italy). Considering the rupture velocity of 3.1 km/s assessed by *Tinti et al.* [2016] for the Amatrice M_w 6.0 earthquake (e.g., similarly, *Liu et al.* [2017] found 3.2 km/s) and our τ_a estimate, from *Kanamori and Rivera* [2004], the resultant $\Delta\tau_s$ is on the order of 30 MPa which in turn corresponds to a Savage-Wood efficiency of 0.69 (i.e., compatible with negative overshoot) [*Beeler et al.*, 2003]. Such a stress drop value is in good agreement with a $\Delta\tau_s$ of 31 MPa estimated through a spectral fitting approach, and using seismological models previously derived for the area [i.e., *Pacor et al.*, 2016] and fixing M_w to 6.0 (see Text S2 for details).

Although the static stress drop shown in Figure 4c is based on Orowan's model, the earthquakes of the 2016 Central Italy sequence are characterized (in relative terms) by significantly larger stress drops than previous sequences in nearby areas (e.g., see the τ_a of ~3 MPa estimated for the L'Aquila 2009 M_w 6.1 and M_L 5.9 in Figure 4c).

The entire fault system where the three 2016 events with $M_w > 5.9$ occurred is constrained at about 7–8 km of depth (i.e., we thus assume similar rigidity and shear wave velocity) and the events had similar focal mechanism [*Gruppo di lavoro INGV*, 2016]. We therefore consider the observed variations in the measured τ_a being indicative of relative different dynamic characteristics (i.e., variations in stress drop and rupture velocity). Our findings indicate that the systematic estimation of the E_R/M_0 ratio for small-to-moderate earthquakes can contribute to the improved understanding of the physics of earthquakes in the Italian region. Additionally, such efforts could improve the resolution of the spatial distribution of seismogenic stress, thus identifying faults which are capable of supporting high stress and could eventually lead to major seismic events.

The IV2 parameter obtained from the whole *P* wave time window for recordings within 100 km is a suitable proxy for the radiated energy of events up to magnitude 7 or 7.5 (see Text S3), depending on the stress drop. Since M_{Le} is based on E_R, it overcomes the saturation problem affecting M_L, as confirmed by the application to the M_w 6.5 Norcia earthquake (M_L = 6.1; M_{Le} = 6.6). On the other hand, since the proposed procedure is designed for the rapid assessment of the earthquake size, a saturation limit for M_{Le} is introduced by the available duration of the *P* waves window.

Acknowledgments

We would like to thank the Editor J. Ritsema and two anonymous reviewers for their comments and suggestions that allowed us to significantly improve the manuscript content and form. We thank Lonn Brown (ISC) that has kindly improved the English and A. Oth (ECGS) for the useful discussion. This research was carried out in the frame of Programme STAR, financially supported by UniNA and Compagnia di San Paolo, and partly supported by the NERA project that allowed Domenico Di Giacomo to visit the University of Naples. The topography of Figure 1a was extracted from the SRTM30_PLUS V11 of *Becker et al.* [2009] and the figure then drawn using the Generic Mapping Tool [*Wessel and Smith*, 1998] software. Data and information have been downloaded from the following sites: INGV network, http://cnt.rm.ingv.it/instruments/network/IV; ESM database, http://esm.mi.ingv.it/; GCMT, www.globalcmt.org; and GFZ-Geofon, http://geofon.gfz-potsdam.de/eqinfo/list.php. We thank all organizations that made data available.

References

Aki, K. (1968), Seismic displacements near a fault, *J. Geophys. Res.*, *73*, 5359–5376, doi:10.1029/JB073i016p05359.

Al Atik, L., A. Abrahamson, J. J. Bommer, F. Scherbaum, F. Cotton, and N. Kuehn (2010), The variability of ground-motion prediction models and its components, *Seismol. Res. Lett.*, *81*(5), 794–801, doi:10.1785/gssrl.81.5.794.

Ameri, G., et al. (2009), The 6 April 2009 M_w 6.3 L'Aquila (Central Italy) earthquake: Strong-motion observations, *Seismol. Res. Lett.*, *80*, 951–966. doi:10.1785/gssrl.80.6.951.

Atkinson, G. M. (1995), Optimal choice of magnitude scales for seismic hazard analysis, *Seismol. Res. Lett. 66*, 1, 51–55, doi:10.1785/gssrl.66.1.51.

Atkinson, G. M., and T. C. Hanks (1995), A high-frequency magnitude scale, *Bull. Seismol. Soc. Am.*, *85*, 825–833.

Baltay, A., T. Hanks, and G. Beroza (2013), Stable stress-drop measurements and their variability: Implications for ground-motion predictions, *Bull. Seismol. Soc. Am.*, *103*, 211–222.

Barani, S., D. Spallarossa, and P. Bazzurro (2009), Disaggregation of probabilistic ground-motion hazard in Italy, BSSA, *Bull. Seismol. Soc. Am.*, *99*, 2638–2661.

Bates, D., M. Mächler, B. Bolker, and S. Walker (2015), Fitting linear mixed-effects models using lme4, *J. Stat. Softw.*, *67*(1), 1–48, doi:10.18637/jss.v067.i01.

Becker, J. J. D., et al. (2009), Global bathymetry and elevation data at 30 arc seconds resolution: SRTM30_PLUS, *Mar. Geod.*, *32*(4), 355–371.

Beeler, N. M., T. F. Wong, and S. H. Hickman (2003), On the expected relationships among apparent stress, static stress drop, effective shear fracture energy, and efficiency, *Bull. Seismol. Soc. Am.*, *93*, 1381–1389.

Beresnev, I. A. (2009), The reality of the scaling law of earthquake-source spectra?, *J. Seismol.*, *13*, 433–436, doi:10.1007/s10950-008-9136-9.

Bindi, D., R. R. Castro, G. Franceschina, L. Luzi, and F. Pacor (2004), The 1997–1998 Umbria-Marche sequence (central Italy): Source, path and site effects estimated from strong motion data recorded in the epicentral area, *J. Geophys. Res.*, *109*, B04312, doi:10.1029/2003JB002857.

Bindi, D., S. Parolai, H. Grosser, C. Milkereit, and E. Durukal (2007), Empirical ground-motion prediction equations for north western Turkey using the aftershocks of the 1999 Kocaeli earthquake, *Geophys. Res. Lett.*, *34*, L08305, doi:10.1029/2007GL029222.

Bindi, D., Pacor F., Luzi L., Massa M., and G. Ameri (2009), The M_w 6.3, 2009 L'Aquila earthquake: Source, path and site effects from spectral analysis of strong motion data, *Geophys. J. Int.*, *179*(3), 1573–1579, doi:10.1111/j.1365-246X.2009.04392.x.

Bindi, D., F. Pacor, L. Luzi, R. Puglia, M. Massa, G. Ameri, and R. Paolucci (2011), Ground motion prediction equations derived from the Italian strong motion database, *Bull. Earthq. Eng.*, *9*(6), 1899–1920.

Bormann, P., S. Wendt, and D. Di Giacomo (2013), Seismic sources and source parameters, in *New Manual of Seismological Observatory Practice 2 (NMSOP2)*, edited by Bormann, P., Potsdam, Deutsches GeoForschungsZentrum GFZ, pp. 1–259, doi:10.2312/GFZ.NMSOP-2_ch3.

Brondi, P., M. Picozzi, A. Emolo, A. Zollo, and M. Mucciarelli (2015), Predicting the macroseismic intensity from early radiated *P* wave energy for on-site earthquake early warning in Italy, *J. Geophys. Res. Solid Earth*, *120*, 7174–7189, doi:10.1002/2015JB012367

Brune, J. (1970), Tectonic stress and spectra of seismic shear waves from earthquakes, *J. Geophys. Res.*, *75*, 4997–5009, doi:10.1029/JB075i026p04997.

Castro, R. R., F. Pacor, R. Puglia, G. Ameri, J. Letort, M. Massa, and L. Luzi (2013), The 2012 May 20 and 29, Emilia earthquakes (Northern Italy) and the main aftershocks: *S* wave attenuation, acceleration source functions and site effects, *Geophys. J. Int.*, *195*, 597–611.

Choy, G. L., and J. Boatwright (1995), Global patterns of radiated seismic energy and apparent stress, *J. Geophys. Res.*, *100*, 18,205–18,226, doi:10.1029/95JB01969.

Choy, G. L., and S. Kirby (2004), Apparent stress, fault maturity and seismic hazard for normal-fault earthquakes at subduction zones, *Geophys. J. Int.*, *159*, 991–1012.

Cocco, M., and A. Rovelli (1989), Evidence for the variation of stress drop between normal and thrust faulting earthquakes in Italy, *J. Geophys. Res.*, *94*, 9399–9416, doi:10.1029/89JB00468.

Colombelli, S., O. Amoroso, A. Zollo, and H. Kanamori (2012), Test of a threshold-based earthquake early warning using Japanese data, *Bull. Seismol. Soc. Am.*, *102*, 1266–1275, doi:10.1785/0120110149.

Colombelli, S., A. Zollo, G. Festa, and M. Picozzi (2014), Evidence for a difference in rupture initiation between small and large earthquakes, *Nat. Commun.*, *5*, 3958, doi:10.1038/ncomms4958.

Deichmann, N. (2017), Theoretical basis for the observed break in ML/MW scaling between small and large earthquakes, *Bull. Seismol. Soc. Am.*, *107*, 2, doi:10.1785/0120160318.

Di Giacomo, D., H. Grosser, S. Parolai, P. Bormann, and R. Wang (2008), Rapid determination of M_e for strong to great shallow earthquakes, *Geophys. Res. Lett.*, *35*, L10308, doi:10.1929/2008GL033505.

Di Giacomo, D., S. Parolai, P. Bormann, H. Grosser, J. Saul, R. Wang, and J. Zschau (2010), Suitability of rapid energy magnitude estimations for emergency response purposes, *Geophys. J. Int.*, *180*, 361–374, doi: 10.1111/j.1365-246X.2009.04416.x.

Festa, G., A. Zollo, and M. Lancieri (2008), Earthquake magnitude estimation from early radiated energy, *Geophys. Res. Lett.*, *35*, L22307, doi:10.1029/2008GL035576.

Gruppo di lavoro INGV (2016), Summary report on the October 30, 2016 earthquake in central Italy M_W 6.5. [Available at https://ingvterre-moti.files.wordpress.com/2016/11/en20161108_rapporto_centroitaliadef.pdf.]

Hanks, T. C., and H. Kanamori (1979), A moment magnitude scale, *J. Geophys. Res.*, *84*(5), 2348–2350, doi:10.1029/JB084iB05p02348.

Haskell, N. A. (1964), Total energy and energy spectral density of elastic wave radiation from propagating faults, *Bull. Seismol. Soc. Am.*, *54*, 1811–1841.

Izutani, Y., and H. Kanamori (2001), Scale-dependence of seismic energy-to-moment ratio for strike-slip earthquakes in Japan, *Geophys. Res. Lett.*, *28*, 4007–4010, doi:10.1029/2001GL013402.

Kanamori, H. (1977), The energy release in great earthquakes, *J. Geophys. Res.*, *82*, 2981–2876, doi:10.1029/JB082i020p02981.

Kanamori, H. (1983), Magnitude scale and quantification of earthquakes, *Tectonophysics*, *93*, 185–199.

Kanamori, H. (2005), Real-time seismology and earthquake damage mitigation, *Annu. Rev. Earth Planet. Sci.*, *33*, 195–214, doi:10.1146/annurev.earth.33.092203.122626.

Kanamori, H., and D. L. Anderson (1975), Theoretical basis of some empirical relations in seismology, *Bull. Seismol. Soc. Am.*, *65*, 1073–1095.

Kanamori, H., and E. Brodsky (2004), The physics of earthquakes, *Rep. Prog. Phys.*, *67*(2004), 1429–1496, doi:10.1088/0034-4885/67/8/R03.

Kanamori, H., and L. Rivera (2004), Static and dynamic scaling relations for earthquakes and their implications for rupture speed and stress drop, *Bull. Seismol. Soc. Am.*, *94*(1), 314–319.

Kanamori, H., E. Hauksson, L. K. Hutton, and L. M. Jones (1993), Determination of earthquake energy release and ML using TERRAscope, *Bull. Seismol. Soc. Am.*, *83*, 330–346.

Lancieri, M., A. Fuenzalida, S. Ruiz, and R. Madariaga (2011), Magnitude scaling of early warning parameters for the M_w 7.8 Tocopilla, Chile, earthquake and its aftershocks, *Bull. Seismol. Soc. Am.*, *101*(2), 447–463, doi:10.1785/0120100045.

Lanzano, G., M. D'Amico, C. Felicetta, R. Puglia, L. Luzi, F. Pacor, D. Bindi (2016), Ground-motion prediction equations for region-specific probabilistic seismic-hazard analysis, *Bull. Seismol. Soc. Am.. 106*, 73–92, doi:10.1785/0120150096.

Liu, C., Y. Zheng, Z. Xie, and X. Xiong, (2017), Rupture features of the 2016 M_w 6.2 Norcia earthquake and its possible relationship with strong seismic hazards, *Geophys. Res. Lett.*, *44*, 1320–1328, doi:10.1002/2016GL071958.

Luzi, L., S. Hailmikael, D. Bindi, F. Pacor, F. Mele, and F. Sabetta (2008), ITACA (ITalian ACcelerometric Archive): A web portal for the dissemination of Italian strong motion data, *Seismol. Res. Lett.*, *79*(5), doi:10.1785/gssrl.79.5.

Luzi, L., F. Pacor, G. Ameri, R. Puglia, P. Burrato, M. Massa, P. Augliera, F. Gianlorenzo, S. Lovati, and R. R. Castro Escamilla (2013), Overview on the strong motion data recorded during the May–June 2012 Emilia seismic sequence, *Seismol. Res. Lett.*, *84*(4), 629–644. doi:10.1785/0220120154.

Malagnini, L., L. Scognamiglio, A. Mercuri, A. Akinci, and K. Mayeda (2008), Strong evidence for non-similar earthquake source scaling in central Italy, *Geophys. Res. Lett.*, *35*, L17303, doi:10.1029/2008GL034310.

Malagnini, L., S. Nielsen, K. Mayeda, and E. Boschi (2010), Energy radiation from intermediate- to large-magnitude earthquakes: Implications for dynamic fault weakening, *J. Geophys. Res.*, *115*, B06319, doi:10.1029/2009JB006786.

Mayeda, K., and W. R. Walter (1996), Moment, energy, stress drop, and source spectra of western United States earthquakes from regional coda envelopes, *J. Geophys. Res.*, *101*, 11,195–11,208, doi:10.1029/96JB00112.

Mereu, R. (2017), A note on the ratio of the moment magnitude scale to other magnitude scales: Theory and applications, *Seismol. Res. Lett.*, *88*, doi:10.1785/0220160104.

Orowan, E. (1960), Mechanism of seismic faulting, *Geol. Soc. Am. Mem.*, *79*, 323–345.

Oth, A. (2013), On the characteristics of earthquake stress release variations in Japan. *Earth Planet. Sci. Lett.*, *377-378*, 132–141, doi:10.1016/j.epsl.2013.06.037.

Oth, A., D. Bindi, S. Parolai and D. Di Giacomo (2010), Earthquake scaling characteristics and the scale-(in)dependence of seismic energy-to-moment ratio: Insights from KiK-net data in Japan, *Geophys. Res. Lett.*, *37*, L19304, doi:10.1029/2010GL044572.

Pacor, F., R. Paolucci, G. Ameri, M. Massa, and R. Puglia (2011), Italian strong motion records in ITACA: Overview and record processing, *Bull. Earthq. Eng.*, doi:10.1007/s10518-011-9295-x.

Pacor F., D. Spallarossa, A. Oth, L. Luzi, R. Puglia, L. Cantore, A. Mercuri, M. D'Amico and D. Bindi (2016), Spectral models for ground motion prediction in the L'Aquila region (central Italy): Evidence for stress-drop dependence on magnitude and depth, *Geophys. J. Int.*, *204*(2), 697–718, doi:10.1093/gji/ggv448.

Picozzi, M., A. Zollo, P. Brondi, S. Colombelli, L. Elia, and C. Martino (2015), Exploring the feasibility of a nationwide earthquake early warning system in Italy, *J. Geophys. Res. Solid Earth*, *120*, 2446–2465, doi:10.1002/2014JB011669.

Sato, T., and T. Hirasawa (1973), Body wave spectra from propagating shear cracks, *J. Phys. Earth*, *21*, 415–431.

Satriano, C., L. Elia, C. Martino, M. Lancieri, A. Zollo, and G. Iannacone (2011), PRESTo, the earthquake early warning system for Southern Italy: Concepts, capabilities and future perspectives, *Soil Dyn. Earthq. Eng.*, doi:10.1016/j.soildyn.2010.06.008.

Singh, S. K., and M. Ordaz (1994), Seismic energy release in Mexican Subduction zone earthquakes, *Bull. Seismol. Soc. Am.*, *84*(5), 1533–1550.

Thatcher W., and T. Hanks (1973), Source parameters of southern California earthquakes, *J. Geophys. Res.*, *78*, 8547–8576, doi:10.1029/JB078i035p08547.

Tinti, E., L. Scognamiglio, A. Michelini, and M. Cocco (2016), Slip heterogeneity and directivity of the M_L 6.0, 2016, Amatrice earthquake estimated with rapid finite-fault inversion, *Geophys. Res. Lett.*, *43*, 10,745–10,752, doi:10.1002/2016GL071263.

Wessel, P., and W. H. F. Smith (1998), New, improved version of the Generic Mapping Tool released, *Eos. Trans. AGU*, *79*(47), 579, doi:10.1029/98EO00426.

Zollo, A., M. Lancieri, and S. Nielsen (2006), Earthquake magnitude estimation from peak amplitudes of very early seismic signals on strong motion, *Geophys. Res. Lett.*, *33*, L23312, doi:10.1029/2006GL027795.

Zollo, A., A. Orefice, and V. Convertito (2014), Source parameter scaling and radiation efficiency of microearthquakes along the Irpinia fault zone in southern Apennines, Italy, *J. Geophys. Res. Solid Earth*, *119*, 3256–3275, doi:10.1002/2013JB010116.